

# Branching ratio and $CP$ violation of $B \rightarrow K\pi$ decays in a modified perturbative QCD approach

Ru-Xuan Wang\* and Mao-Zhi Yang†

*School of Physics, Nankai University, Tianjin 300071, P.R. China*

(Dated: December 20, 2022)

We calculate the branching ratio and  $CP$  violations for  $B \rightarrow K\pi$  decays in a modified perturbative QCD approach based on  $k_T$  factorization. The resummation effect of the transverse momentum regulates the endpoint singularity. Using the  $B$  meson wave function that is obtained in the relativistic potential model, soft contribution can not be suppressed effectively by Sudakov factor. Soft scale cutoff and soft  $BK$ ,  $B\pi$  and  $K\pi$  form factors have to be introduced. The most important next-to-leading-order contributions from the vertex corrections, the quark loops, and the magnetic penguins are also considered. In addition, the contribution of the color-octet hadronic matrix element is included which is essentially of long-distance dynamics. Our predictions for branching ratios and  $CP$  violations are in good agreement with the experimental data. Especially the theoretical result of dramatic difference between the  $CP$  violations of  $B^+ \rightarrow K^+\pi^0$  and  $B^0 \rightarrow K^+\pi^-$  is consistent with experimental measurement, therefore the  $K\pi$  puzzle in  $B$  decays can be resolved in our way of the modified perturbative QCD approach.

PACS numbers: 12.38.Bx, 12.39.St, 13.25.Hw

## I. INTRODUCTION

Over the past twenty years, there has been a great deal of interest in  $B \rightarrow K\pi$  decays. From  $B$  factory experiments, a large amount of data about  $B$  decays has been collected. The precise data revealed significant difference between experiment measurements and theoretical predictions. For  $B \rightarrow K\pi$  decays, the expected  $CP$  violations of  $B^+ \rightarrow K^+\pi^0$  and  $B^0 \rightarrow K^+\pi^-$  decays are roughly equal from the theoretical point of view [1, 2]. The branching ratios and  $CP$  violations of  $B \rightarrow K\pi$  decays measured by experiment are [3]

$$\begin{aligned} B(B^+ \rightarrow K^0\pi^+) &= (2.37 \pm 0.08) \times 10^{-5}, \\ B(B^+ \rightarrow K^+\pi^0) &= (1.29 \pm 0.05) \times 10^{-5}, \\ B(B^0 \rightarrow K^+\pi^-) &= (1.96 \pm 0.05) \times 10^{-5}, \\ B(B^0 \rightarrow K^0\pi^0) &= (9.9 \pm 0.5) \times 10^{-6}, \end{aligned} \quad (1)$$

and

$$\begin{aligned} A_{CP}(B^+ \rightarrow K^0\pi^+) &= -0.017 \pm 0.016, \\ A_{CP}(B^+ \rightarrow K^+\pi^0) &= 0.037 \pm 0.021, \\ A_{CP}(B^0 \rightarrow K^+\pi^-) &= -0.083 \pm 0.004, \\ A_{CP}(B^0 \rightarrow K^0\pi^0) &= 0.00 \pm 0.13. \end{aligned} \quad (2)$$

One can obtain  $\Delta A_{CP} \equiv A_{CP}(B^+ \rightarrow K^+\pi^0) - A_{CP}(B^0 \rightarrow K^+\pi^-) = 0.120 \pm 0.021$  from the data given in Eq. (2). The difference deviates from zero by more than  $5\sigma$ . This is what is called  $B \rightarrow K\pi$  puzzle.

To solve the  $K\pi$  puzzle in  $B$  decays, the next-to-leading-order QCD corrections have been taken into account in perturbative QCD (PQCD) approach in Refs.

[2, 4]. A soft factor that enhances the nonfactorizable amplitudes has been introduced based on the analysis of soft divergences that appear in higher order loop corrections in QCD in Refs. [5, 6]. There are also works where new physics effects are considered to solve the  $K\pi$  puzzle [7, 8]. All of them can reduce the discrepancy between theoretical prediction and experimental data, but the agreement of the theoretical prediction and the data is still not satisfactory. So the  $K\pi$  puzzle is still not completely solved.

In this work we study  $B \rightarrow K\pi$  decays in a modified perturbative QCD (PQCD) approach, with which  $B \rightarrow \pi\pi$  decays have been studied very recently in Ref. [9], where both the branching ratios and  $CP$  violation in three  $B \rightarrow \pi\pi$  decay modes are well consistent with experimental data. It is found that, using  $B$  meson wave function that obtained by solving the bound state equation in relativistic potential model [10–14], the suppression to soft contribution from Sudakov factor is not large enough. A soft truncation have to be introduced in an appropriate momentum scale. When the momentum transfer larger than this critical momentum scale, the contributions to  $B \rightarrow \pi$  and  $B \rightarrow K$  transition form factors can be calculated perturbatively. And soft form factors need to be introduced to include soft contributions with the momentum transfer lower than the momentum scale of cutoff. With the soft cutoff and soft form factors, the calculation of  $B \rightarrow \pi$  and  $B \rightarrow K$  transition form factors becomes more reliable.

The branching ratios and  $CP$  violations of  $B \rightarrow K\pi$  decays are calculated in this work. The amplitudes are treated perturbatively when the momentum transfer larger than the soft cutoff scale. We also consider the important next-to-leading-order contributions of hard part from the vertex corrections, the quark loops and the magnetic penguin. As for the soft part with momentum transfer lower than the cutoff scale, we introduce the  $BK$

\* wangrx@mail.nankai.edu.cn

† yangmz@nankai.edu.cn

and  $B\pi$  transition, and  $K\pi$  production soft form factors. These factors are nonperturbative input parameters. To improve the consistency between theoretical calcualtion and experimental data, we find the nonzero color-octet matrix element  $\langle K\pi|(\bar{s}T^a q)(\bar{q}T^a b)|B\rangle$ , which is derived from the analysis of color structure of quark-antiquark current operators, is necessary. With the appropriate input parameters, our prediction of branching ratio and  $CP$  violation is well consistent with the experiment.

The paper is orginized as follows. The perturbative calculation of leading order contributions of  $B \rightarrow K\pi$  decays are presented in Sec. II. The important next-to-leading order contributions are considered in Sec. III. The contributions of nonperturbative parameters are investigated in Sec. IV and V. The numerical results are shown in Sec. VI. We conclude the analysis in Sec. VII.

## II. THE HARD AMPLITUDES OF LEADING ORDER CONTRIBUTIONS IN PERTURBATIVE QCD

When the momentum transfer in the transition process is larger than the cutoff scale  $\mu_c$ , which is used to separate the contributions of hard and soft parts, the decay amplitude can be treated perturbatively. Typically, the critical scale  $\mu_c$  is approximately equal to 1.0 GeV. In perturbative QCD approach, if  $B$  meson decays into two light mesons, the process is dominated by one hard gluon exchanged diagrams. The decay amplitudes can be arranged as the convolution of hard scattering process and meson wave functions

$$\mathcal{M} = \int d^3 k_1 \int d^3 k_2 \int d^3 k_3 \Phi^B(k_1, \mu) C(\mu) \times H(k_1, k_2, k_3, \mu) \Phi^\pi(k_2, \mu) \Phi^K(k_3, \mu), \quad (3)$$

where  $H$  contains the hard scattering dynamics which is calculable using perturbation theory,  $C(t)$ 's are Wilson coefficients,  $\Phi(x)^{B, \pi, K}$  are meson light-cone distribution amplitudes that absorb nonperturbative interactions related to meson states.

For the  $b \rightarrow s$  transntion, the effective Hamiltonian is given by [15]

$$H_{\text{eff}} = \frac{G_F}{\sqrt{2}} \left[ V_u (C_1 O_1^u + C_2 O_2^u) - V_t \left( \sum_{i=3}^{10} C_i O_i + C_{8g} O_{8g} \right) \right], \quad (4)$$

where  $V_u = V_{ub} V_{us}^*$  and  $V_t = V_{tb} V_{ts}^*$ , are CKM matrix elements,  $G_F = 1.16639 \times 10^{-5}$  GeV $^{-2}$  Fermi constant, and the  $C_i$ 's Wilson coefficients. The operators  $O_i$  in the effective Hamiltonian are

$$\begin{aligned} O_1^u &= (\bar{s}_\alpha \gamma^\mu (1 - \gamma_5) u_\beta) (\bar{u}_\beta \gamma_\mu (1 - \gamma_5) b_\alpha), \\ O_2^u &= (\bar{s}_\alpha \gamma^\mu (1 - \gamma_5) u_\alpha) (\bar{u}_\beta \gamma_\mu (1 - \gamma_5) b_\beta), \end{aligned} \quad (5)$$

$$\begin{aligned} O_3 &= (\bar{s}_\alpha \gamma^\mu (1 - \gamma_5) b_\alpha) \sum_{q'} (\bar{q}'_\beta \gamma_\mu (1 - \gamma_5) q'_\beta), \\ O_4 &= (\bar{s}_\alpha \gamma^\mu (1 - \gamma_5) b_\beta) \sum_{q'} (\bar{q}'_\beta \gamma_\mu (1 - \gamma_5) q'_\alpha), \\ O_5 &= (\bar{s}_\alpha \gamma^\mu (1 - \gamma_5) b_\alpha) \sum_{q'} (\bar{q}'_\beta \gamma_\mu (1 + \gamma_5) q'_\beta), \end{aligned} \quad (6)$$

$$\begin{aligned} O_6 &= (\bar{s}_\alpha \gamma^\mu (1 - \gamma_5) b_\beta) \sum_{q'} (\bar{q}'_\beta \gamma_\mu (1 + \gamma_5) q'_\alpha), \\ O_7 &= \frac{3}{2} (\bar{s}_\alpha \gamma^\mu (1 - \gamma_5) b_\alpha) \sum_{q'} e_{q'} (\bar{q}'_\beta \gamma_\mu (1 + \gamma_5) q'_\beta), \\ O_8 &= \frac{3}{2} (\bar{s}_\alpha \gamma^\mu (1 - \gamma_5) b_\beta) \sum_{q'} e_{q'} (\bar{q}'_\beta \gamma_\mu (1 + \gamma_5) q'_\alpha), \\ O_9 &= \frac{3}{2} (\bar{s}_\alpha \gamma^\mu (1 - \gamma_5) b_\alpha) \sum_{q'} e_{q'} (\bar{q}'_\beta \gamma_\mu (1 - \gamma_5) q'_\beta), \\ O_{10} &= \frac{3}{2} (\bar{s}_\alpha \gamma^\mu (1 - \gamma_5) b_\beta) \sum_{q'} e_{q'} (\bar{q}'_\beta \gamma_\mu (1 - \gamma_5) q'_\alpha), \end{aligned} \quad (7)$$

$$O_{8g} = \frac{g_s}{8\pi^2} m_b \bar{s}_\alpha \sigma^{\mu\nu} (1 + \gamma_5) T_{\alpha\beta}^a G_{\mu\nu}^a b_\beta, \quad (8)$$

where  $\alpha$  and  $\beta$  are the color indices. The summation of  $q'$  runs through  $u, d, s, c$ , and  $b$  quarks.

The matrix element  $\langle 0 | \bar{q}_\beta(z) [z, 0] b_\alpha(0) | \bar{B} \rangle$  can be used to define the  $B$  meson wave function

$$\langle 0 | \bar{q}_\beta(z) [z, 0] b_\alpha(0) | \bar{B} \rangle = \int d^3 k \Phi_{\alpha\beta}^B(\vec{k}) \exp(-ik \cdot z), \quad (9)$$

where  $[z, 0]$  represents the path-ordered exponential

$$[z, 0] = \mathcal{P} \exp \left[ -ig_s T^a \int_0^1 dz z^\mu A_\mu^a(\alpha z) \right]. \quad (10)$$

We use the  $B$  wave function that is obtained by solving bound-state equation in the QCD-inspired relativistic potential model [10–13], where the mass spectrum and decay constants of  $b$ -flavored meson system calculated simultaneously with the wave functions, are consistent with experimental data.

In the rest-frame of  $B$  meson, the spinor wave function  $\Phi_{\alpha\beta}^B(\vec{k})$  is given by [13]

$$\begin{aligned} \Phi_{\alpha\beta}^B(\vec{k}) &= \frac{-if_B m_B}{4} K(\vec{k}) \\ &\times \left\{ (E_Q + m_Q) \frac{1+\not{k}}{2} \left[ \left( \frac{k_+}{\sqrt{2}} + \frac{m_q}{2} \right) \not{h}_+ \right. \right. \\ &+ \left( \frac{k_-}{\sqrt{2}} + \frac{m_q}{2} \right) \not{h}_- - k_\perp^\mu \gamma_\mu \left. \right] \gamma_5 \\ &- (E_q + m_q) \frac{1-\not{k}}{2} \left[ \left( \frac{k_+}{\sqrt{2}} - \frac{m_q}{2} \right) \not{h}_+ \right. \\ &+ \left. \left. \left( \frac{k_-}{\sqrt{2}} - \frac{m_q}{2} \right) \not{h}_- - k_\perp^\mu \gamma_\mu \right] \gamma_5 \right\}_{\alpha\beta}, \end{aligned} \quad (11)$$

where  $Q$  and  $q$  represent the heavy and light quarks in  $B$  meson ( $b\bar{q}$ ), respectively.  $v$  is the four-speed of  $B$  meson which satisfies  $p_B^\mu = m_B v^\mu$  and  $v^\mu = (1, 0, 0, 0)$ , and  $k$  is the momentum of the light quark in the rest frame of the meson.  $k^\pm$  and  $k_\perp$  are defined by

$$k^\pm = \frac{E_q \pm k^3}{\sqrt{2}}, \quad k_\perp^\mu = (0, k^1, k^2, 0). \quad (12)$$

$n_\pm^\mu$  are two light-like vectors with  $n_\pm^\mu = (1, 0, 0, \mp 1)$ , and  $K(\vec{k})$  is the function proportional to the  $B$ -meson wave function

$$K(\vec{k}) = \frac{2N_B \Psi_0(\vec{k})}{\sqrt{E_q E_Q (E_q + m_q)(E_Q + m_Q)}}, \quad (13)$$

with the normalization constant  $N_B = \frac{1}{f_B} \sqrt{\frac{3}{(2\pi)^3 m_B}}$  and the  $B$  meson wave function

$$\Psi_0(\vec{k}) = a_1 e^{a_2 |\vec{k}|^2 + a_3 |\vec{k}| + a_4}, \quad (14)$$

where the parameters are [13]

$$\begin{aligned} a_1 &= 4.55_{-0.30}^{+0.40} \text{ GeV}^{-3/2}, \\ a_2 &= -0.39_{-0.20}^{+0.15} \text{ GeV}^{-2}, \\ a_3 &= -1.55 \pm 0.20 \text{ GeV}^{-1}, \\ a_4 &= -1.10_{-0.05}^{+0.10}. \end{aligned} \quad (15)$$

In  $B \rightarrow K\pi$  decays, the mass difference of  $B$  and final state mesons is large. The momenta of the outgoing  $K$  and  $\pi$  mesons are large, so the wave functions of light mesons can be defined on the light-cone [18–20]

$$\begin{aligned} \langle \pi(p) | \bar{q}_\delta(x) q'_\gamma(0) | 0 \rangle \\ = \int du d^2 k_{q\perp} \Phi_{\gamma\delta}^\pi \exp [i(u p \cdot x - x_\perp \cdot k_{q\perp})], \end{aligned} \quad (16)$$

with the spinor wave function  $\Phi_{\gamma\delta}^\pi$  being

$$\begin{aligned} \Phi_{\gamma\delta}^\pi &= \frac{if_\pi}{4} \left[ \not{p} \gamma_5 \phi_\pi(u, k_{q\perp}) - \mu_\pi \gamma_5 \phi_P^\pi(u, k_{q\perp}) \right. \\ &\quad \left. + \mu_\pi \gamma_5 \sigma^{\mu\nu} p_\mu z_\nu \frac{\phi_\sigma^\pi(u, k_{q\perp})}{6} \right]_{\gamma\delta}, \end{aligned} \quad (17)$$

where  $f_\pi$  is pion decay constant, and  $\mu_\pi$  is the chiral parameter with

$$\mu_\pi = m_\pi^2 / (m_u + m_d). \quad (18)$$

$\phi_\pi$ ,  $\phi_P^\pi$  and  $\phi_\sigma^\pi$  are the twist-2 and twist-3 light-cone distribution amplitudes. In momentum space, the pion wave function can be expressed as

$$\begin{aligned} \Phi_{\gamma\delta}^\pi &= \frac{if_\pi}{4} \left[ \not{p} \gamma_5 \phi_\pi(u, k_{q\perp}) - \mu_\pi \gamma_5 \phi_P^\pi(u, k_{q\perp}) \right. \\ &\quad \left. + \mu_\pi \gamma_5 i \sigma^{\mu\nu} \frac{p_\mu \bar{p}_\nu}{p \cdot \bar{p}} \frac{1}{6} \frac{\partial \phi_\sigma^\pi(u, k_{q\perp})}{\partial u} \right. \\ &\quad \left. - \mu_\pi \gamma_5 i \sigma^{\mu\nu} p_\mu \frac{\phi_\sigma^\pi(u, k_{q\perp})}{6} \frac{\partial}{\partial k_{q\perp\nu}} \right]_{\gamma\delta}, \end{aligned} \quad (19)$$

where  $\bar{p}$  is the momentum with the moving direction opposite to that of pion and the energy the same. For the wave function of  $K$  meson, one can get it by just replacing the distribution amplitudes of pion with that of the kaon [20].

There are eight diagrams contributing to  $B \rightarrow K\pi$  decays in leading order in QCD which are shown in Fig. 1. During the calculation, we keep the transverse momentum of quarks and gluons. At the endpoint region, i.e., when the momentum fraction of parton  $x \rightarrow 0$ , the transverse momentum cannot be neglected. We encounter double logarithm divergence such as  $\alpha_s(\mu) \ln^2 k_\perp / \mu$  when soft and collinear divergences overlap. This large double logarithms should be resummed into the Sudakov factor [21, 22]. In addition, there are other double logarithms such as  $\alpha_s(\mu) \ln^2 x$  from the QCD corrections of the weak vertex. This double logarithm can also be resummed into the threshold factor [23]. The Sudakov factor and threshold factor suppress the endpoint singularity and improve

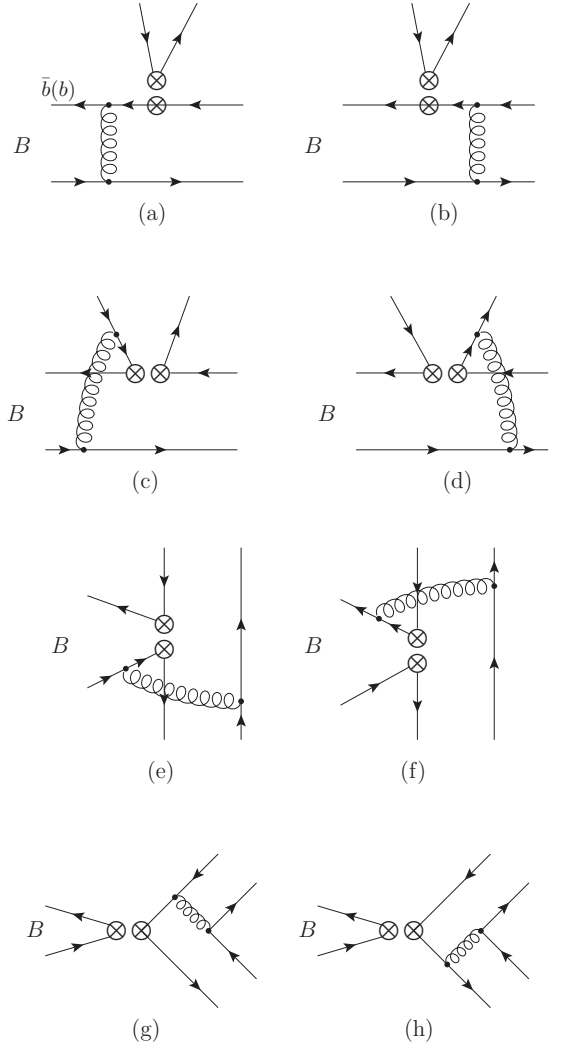


FIG. 1. Diagrams which are contributing to the  $B \rightarrow K\pi$  decays.

the reliability of the calculation of  $B$  decays in PQCD approach. For convenience, we perform the calculation of the decay amplitudes in  $b$ -space where  $b$  is the conjugate variable of transverse momentum  $k_{\perp}$ .

The diagrams (a) and (b) in Fig. 1 are factorizable diagrams. Fig. 1 (c) and (d) are nonfactorizable diagrams, (e) and (f) nonfactorizable annihilation diagrams, and (g)

and (h) factorizable annihilation diagrams. The symbol of the circled times in these diagrams stands for four-quark operator insertion which are given in Eqs. (5)–(8).

Firstly, we calculate the diagrams (a) and (b). If the meson which is factorized out is kaon in diagrams (a) and (b), the contribution with the  $(V - A)(V - A)$  operators inserted is

$$\begin{aligned}
F_e = & 2\pi^2 f_B f_{\pi} m_B^2 \frac{C_F}{N_c} \int k_{1\perp} dk_{1\perp} \int_{x_1^d}^{x_1^u} dx_1 \int_0^1 dx_3 \int_0^\infty b_1 db_1 b_3 db_3 \left( \frac{1}{2} m_B + \frac{|\mathbf{k}_{1\perp}|^2}{2x_1^2 m_B} \right) K(\vec{k}_1) (E_Q + m_Q) \\
& \times J_0(k_{1\perp} b_1) \left\{ \alpha_s(t_e^1) \left[ \left( (x_3 - 2) E_q - x_3 k_1^3 \right) \phi_{\pi}(x_3, b_3) + r_{\pi} \left( (1 - 2x_3) E_q + k_1^3 \right) \phi_P^\pi(x_3, b_3) - \frac{1}{6} r_{\pi} \right. \right. \\
& \times \left. \left. \left( (1 - 2x_3) E_q + k_1^3 \right) \phi_{\sigma}'^\pi(x_3, b_3) \right] h_e(x_1, 1 - x_3, b_1, b_3) S_t(x_3) \exp[-S_B(t_e^1) - S_{\pi}(t_e^1)] + \alpha_s(t_e^2) 2r_{\pi} \right. \\
& \times \left. \left. (-E_q + k_1^3) \phi_P^\pi(x_3, b_3) h_e(1 - x_3, x_1, b_3, b_1) S_t(x_1) \exp[-S_B(t_e^2) - S_{\pi}(t_e^2)] \right\}. \right. \tag{20}
\end{aligned}$$

The contribution related to the  $(S + P)(S - P)$  operators which come from Fierz transformation of  $(V - A)(V + A)$  operators is

$$\begin{aligned}
F_e^P = & 2\pi^2 f_B f_{\pi} m_B^2 \frac{C_F}{N_c} \int k_{1\perp} dk_{1\perp} \int_{x_1^d}^{x_1^u} dx_1 \int_0^1 dx_3 \int_0^\infty b_1 db_1 b_3 db_3 \left( \frac{1}{2} m_B + \frac{|\mathbf{k}_{1\perp}|^2}{2x_1^2 m_B} \right) K(\vec{k}_1) (E_Q + m_Q) \\
& \times J_0(k_{1\perp} b_1) 2r_K \left\{ \alpha_s(t_e^1) \left[ -(E_q + k_1^3) \phi_{\pi}(x_3, b_3) + r_{\pi} \left( (x_3 - 3) E_q + (1 - x_3) k_1^3 \right) \phi_P^\pi(x_3, b_3) + \frac{1}{6} r_{\pi} \right. \right. \\
& \times \left. \left. \left( (x_3 - 1) E_q - (1 + x_3) k_1^3 \right) \phi_{\sigma}'^\pi(x_3, b_3) \right] h_e(x_1, 1 - x_3, b_1, b_3) S_t(x_3) \exp[-S_B(t_e^1) - S_{\pi}(t_e^1)] \right. \\
& \left. + \alpha_s(t_e^2) 2r_{\pi} (-E_q + k_1^3) \phi_P^\pi(x_3, b_3) h_e(1 - x_3, x_1, b_3, b_1) S_t(x_1) \exp[-S_B(t_e^2) - S_{\pi}(t_e^2)] \right\}. \tag{21}
\end{aligned}$$

If the meson factorized out is pion in diagrams (a) and (b), the contributions from this two diagrams with the  $(V - A)(V - A)$  and  $(V - A)(V + A)$  operators inserted are

$$\begin{aligned}
F_{eK} = & 2\pi^2 f_B f_K m_B^2 \frac{C_F}{N_c} \int k_{1\perp} dk_{1\perp} \int_{x_1^d}^{x_1^u} dx_1 \int_0^1 dx_2 \int_0^\infty b_1 db_1 b_2 db_2 \left( \frac{1}{2} m_B + \frac{|\mathbf{k}_{1\perp}|^2}{2x_1^2 m_B} \right) K(\vec{k}_1) (E_Q + m_Q) \\
& \times J_0(k_{1\perp} b_1) \left\{ \alpha_s(t_{eK}^1) \left[ \left( (x_2 - 2) E_q + x_2 k_1^3 \right) \phi_K(x_2, b_2) + r_K \left( (1 - 2x_2) E_q - k_1^3 \right) \phi_P^K(x_2, b_2) - \frac{1}{6} r_K \right. \right. \\
& \times \left. \left. \left( (1 - 2x_2) E_q - k_1^3 \right) \phi_{\sigma}'^K(x_2, b_2) \right] h_e(x_1, 1 - x_2, b_1, b_2) S_t(x_2) \exp[-S_B(t_{eK}^1) - S_K(t_{eK}^1)] + \alpha_s(t_{eK}^2) \right. \\
& \times \left. 2r_K (-E_q - k_1^3) \phi_P^K(x_2, b_2) h_e(1 - x_2, x_1, b_2, b_1) S_t(x_1) \exp[-S_B(t_{eK}^2) - S_K(t_{eK}^2)] \right\}, \tag{22}
\end{aligned}$$

and

$$F_{eK}^P = -F_{eK}. \tag{23}$$

There are also factorizable annihilation diagrams (g) and (h), where the  $B$  meson is factored out. The results of

diagrams (g) and (h) are

$$\begin{aligned}
F_a = & 2\pi f_K f_\pi m_B^2 \frac{C_F}{N_c} \int_0^1 dx_2 dx_3 \int_0^\infty b_2 db_2 b_3 db_3 \left\{ \alpha_s(t_a^1) \left[ x_3 \phi_K(x_2, b_2) \phi_\pi(x_3, b_3) + 2r_K r_\pi (1+x_3) \phi_P^K(x_2, b_2) \right. \right. \\
& \times \phi_P^\pi(x_3, b_3) - \frac{1}{3} r_K r_\pi (1-x_3) \phi_P^K(x_2, b_2) \phi_\sigma'^\pi(x_3, b_3) \left. \right] h_a(1-x_2, x_3, b_2, b_3) S_t(x_3) \exp[-S_K(t_a^1) - S_\pi(t_a^1)] \\
& + \alpha_s(t_a^2) \left[ -(1-x_2) \phi_K(x_2, b_2) \phi_\pi(x_3, b_3) - 2r_K r_\pi (2-x_2) \phi_P^K(x_2, b_2) \phi_P^\pi(x_3, b_3) - \frac{1}{3} r_K r_\pi x_2 \phi_\sigma'^K(x_2, b_2) \right. \\
& \times \phi_P^\pi(x_3, b_3) \left. \right] h_a(x_3, 1-x_2, b_3, b_2) S_t(x_2) \exp[-S_K(t_a^2) - S_\pi(t_a^2)] \left. \right\}, \tag{24}
\end{aligned}$$

$$\begin{aligned}
F_a^P = & 4\pi f_K f_\pi m_B^2 \frac{C_F}{N_c} \chi_B \int_0^1 dx_2 dx_3 \int_0^\infty b_2 db_2 b_3 db_3 \left\{ \alpha_s(t_a^1) \left[ -r_\pi x_3 \phi_K(x_2, b_2) \phi_P^\pi(x_3, b_3) + \frac{1}{6} r_\pi x_3 \phi_K(x_2, b_2) \right. \right. \\
& \times \phi_\sigma'^\pi(x_3, b_3) - 2r_K \phi_P^K(x_2, b_2) \phi_\pi(x_3, b_3) \left. \right] h_a(1-x_2, x_3, b_2, b_3) S_t(x_3) \exp[-S_K(t_a^1) - S_\pi(t_a^1)] + \alpha_s(t_a^2) \\
& \times \left[ -2r_\pi \phi_K(x_2, b_2) \phi_P^\pi(x_3, b_3) - r_K (1-x_2) \phi_P^K(x_2, b_2) \phi_\pi(x_3, b_3) - \frac{1}{6} r_K (1-x_2) \phi_\sigma'^K(x_2, b_2) \phi_\pi(x_3, b_3) \right] \\
& \times h_a(x_3, 1-x_2, b_3, b_2) S_t(x_2) \exp[-S_K(t_a^2) - S_\pi(t_a^2)] \left. \right\}. \tag{25}
\end{aligned}$$

As for the nonfactorizable diagrams (c), (d), (e) and (f), the amplitudes involve all three meson wave functions. The integral over  $b$  using  $\delta$  function is necessary. The amplitudes of the nonfactorizable emission diagrams (c) and (d) are

$$\begin{aligned}
\mathcal{M}_e = & 2\pi^2 f_B f_K f_\pi m_B^2 \frac{C_F}{N_c} \int k_{1\perp} dk_{1\perp} \int_{x_1^d}^{x_1^u} dx_1 \int_0^1 dx_2 dx_3 \int_0^\infty b_1 db_1 b_2 db_2 \left( \frac{1}{2} m_B + \frac{|\mathbf{k}_{1\perp}|^2}{2x_1^2 m_B} \right) K(\vec{k}_1) (E_Q + m_Q) \\
& \times J_0(k_{1\perp} b_1) \phi_K(x_2, b_2) \left\{ \alpha_s(t_d^1) \left[ -x_2 (E_q + k_1^3) \phi_\pi(x_3, b_1) + r_\pi (1-x_3) (E_q - k_1^3) \phi_P^\pi(x_3, b_1) + \frac{1}{6} r_\pi (1-x_3) \right. \right. \\
& \times (E_q - k_1^3) \phi_\sigma'^\pi(x_3, b_1) \left. \right] h_d(x_1, x_2, 1-x_3, b_1, b_2) S_t(x_3) \exp[-S_B(t_d^1) - S_K(t_d^1) - S_\pi(t_d^1)|_{b_3 \rightarrow b_1}] + \alpha_s(t_d^2) \\
& \times \left[ \left( (2-x_2-x_3) E_q - (x_2-x_3) k_1^3 \right) \phi_\pi(x_3, b_1) - r_\pi (1-x_3) (E_q + k_1^3) \phi_P^\pi(x_3, b_1) + \frac{1}{6} r_\pi (1-x_3) (E_q + k_1^3) \right. \\
& \times \phi_\sigma'^\pi(x_3, b_1) \left. \right] h_d(x_1, 1-x_2, 1-x_3, b_1, b_2) S_t(x_3) \exp[-S_B(t_d^2) - S_K(t_d^2) - S_\pi(t_d^2)|_{b_3 \rightarrow b_1}] \left. \right\}, \tag{26}
\end{aligned}$$

$$\begin{aligned}
\mathcal{M}_e^P = & 2\pi^2 f_B f_K f_\pi m_B^2 \frac{C_F}{N_c} \int k_{1\perp} dk_{1\perp} \int_{x_1^d}^{x_1^u} dx_1 \int_0^1 dx_2 dx_3 \int_0^\infty b_1 db_1 b_2 db_2 \left( \frac{1}{2} m_B + \frac{|\mathbf{k}_{1\perp}|^2}{2x_1^2 m_B} \right) K(\vec{k}_1) (E_Q + m_Q) \\
& \times J_0(k_{1\perp} b_1) r_K \left\{ \alpha_s(t_d^1) \left[ -x_2 (E_q + k_1^3) \phi_P^K(x_2, b_2) \phi_\pi(x_3, b_1) - r_\pi \left( (1+x_2-x_3) E_q - (1-x_2-x_3) k_1^3 \right) \right. \right. \\
& \times \phi_P^K(x_2, b_2) \phi_P^\pi(x_3, b_1) - \frac{1}{6} r_\pi \left( -(1-x_2-x_3) E_q + (1+x_2-x_3) k_1^3 \right) \phi_P^K(x_2, b_2) \phi_\sigma'^\pi(x_3, b_1) + \frac{1}{6} x_2 \\
& \times (E_q + k_1^3) \phi_\sigma'^K(x_2, b_2) \phi_\pi(x_3, b_1) + \frac{1}{6} r_\pi \left( -(1-x_2-x_3) E_q + (1+x_2-x_3) k_1^3 \right) \phi_\sigma'^K(x_2, b_2) \phi_P^\pi(x_3, b_1) \\
& + \frac{1}{36} r_\pi \left( (1+x_2-x_3) E_q - (1-x_2-x_3) k_1^3 \right) \phi_\sigma'^K(x_2, b_2) \phi_\sigma'^\pi(x_3, b_1) \left. \right] h_d(x_1, x_2, 1-x_3, b_1, b_2) S_t(x_3) \\
& \times \exp[-S_B(t_d^1) - S_K(t_d^1) - S_\pi(t_d^1)|_{b_3 \rightarrow b_1}] + \alpha_s(t_d^2) \left[ (1-x_2) (E_q + k_1^3) \phi_P^K(x_2, b_2) \phi_\pi(x_3, b_1) + r_\pi \right. \\
& \times \left( (2-x_2-x_3) E_q - (x_2-x_3) k_1^3 \right) \phi_P^K(x_2, b_2) \phi_P^\pi(x_3, b_1) + \frac{1}{6} r_\pi \left( -(x_2-x_3) E_q + (2-x_2-x_3) k_1^3 \right) \\
& \times \phi_P^K(x_2, b_2) \phi_\sigma'^\pi(x_3, b_1) + \frac{1}{6} (1-x_2) (E_q + k_1^3) \phi_\sigma'^K(x_2, b_2) \phi_\pi(x_3, b_1) + \frac{1}{6} r_\pi \left( -(x_2-x_3) E_q \right. \\
& \left. \left. \right. \right. \right. \right. \tag{27}
\end{aligned}$$

$$\begin{aligned}
& + (2 - x_2 - x_3)k_1^3 \Big) \phi_\sigma'^K(x_2, b_2) \phi_P^\pi(x_3, b_1) + \frac{1}{36} r_\pi \Big( (2 - x_2 - x_3)E_q - (x_2 - x_3)k_1^3 \Big) \phi_\sigma'^K(x_2, b_2) \\
& \times \phi_\sigma'^\pi(x_3, b_1) \Big] h_d(x_1, 1 - x_2, 1 - x_3, b_1, b_2) S_t(x_3) \exp[-S_B(t_d^2) - S_K(t_d^2) - S_\pi(t_d^2)|_{b_3 \rightarrow b_1}] \Big\},
\end{aligned}$$

$$\begin{aligned}
\mathcal{M}_{eK} = & 2\pi^2 f_B f_K f_\pi m_B^2 \frac{C_F}{N_c} \int k_{1\perp} dk_{1\perp} \int_{x_1^d}^{x_1^u} dx_1 \int_0^1 dx_2 dx_3 \int_0^\infty b_1 db_1 b_3 db_3 \left( \frac{1}{2} m_B + \frac{|\mathbf{k}_{1\perp}|^2}{2x_1^2 m_B} \right) K(\vec{k}_1) \\
& \times (E_Q + m_Q) J_0(k_{1\perp} b_1) \phi_\pi(x_3, b_3) \left\{ \alpha_s(t_{dK}^1) \left[ -x_3(E_q - k_1^3) \phi_K(x_2, b_1) + r_K(1 - x_2)(E_q + k_1^3) \phi_P^K(x_2, b_1) \right. \right. \\
& + \frac{1}{6} r_K(1 - x_2)(E_q + k_1^3) \phi_\sigma'^K(x_2, b_1) \Big] h_d(x_1, x_3, 1 - x_2, b_1, b_3) S_t(x_2) \exp[-S_B(t_{dK}^1) - S_K(t_{dK}^1)|_{b_2 \rightarrow b_1} \\
& - S_\pi(t_{dK}^1)] + \alpha_s(t_{dK}^2) \left[ \left( (2 - x_2 - x_3)E_q - (x_2 - x_3)k_1^3 \right) \phi_K(x_2, b_1) - r_K(1 - x_2)(E_q - k_1^3) \phi_P^K(x_2, b_1) \right. \\
& + \frac{1}{6} r_K(1 - x_2)(E_q - k_1^3) \phi_\sigma'^K(x_2, b_1) \Big] h_d(x_1, 1 - x_3, 1 - x_2, b_1, b_3) S_t(x_2) \exp[-S_B(t_{dK}^2) \\
& \left. \left. - S_K(t_{dK}^2)|_{b_2 \rightarrow b_1} - S_\pi(t_{dK}^2) \right] \right\}, \tag{28}
\end{aligned}$$

$$\begin{aligned}
\mathcal{M}_{eK}^P = & 2\pi^2 f_B f_K f_\pi m_B^2 \frac{C_F}{N_c} \int k_{1\perp} dk_{1\perp} \int_{x_1^d}^{x_1^u} dx_1 \int_0^1 dx_2 dx_3 \int_0^\infty b_1 db_1 b_3 db_3 \left( \frac{1}{2} m_B + \frac{|\mathbf{k}_{1\perp}|^2}{2x_1^2 m_B} \right) K(\vec{k}_1) \\
& \times (E_Q + m_Q) J_0(k_{1\perp} b_1) \phi_\pi(x_3, b_3) \left\{ \alpha_s(t_{dK}^1) \left[ \left( (1 - x_2 + x_3)E_q + (1 - x_2 - x_3)k_1^3 \right) \phi_K(x_2, b_1) - r_K \right. \right. \\
& \times (1 - x_2)(E_q - k_1^3) \phi_P^K(x_2, b_1) + \frac{1}{6} r_K(1 - x_2)(E_q - k_1^3) \phi_\sigma'^K(x_2, b_1) \Big] h_d(x_1, x_3, 1 - x_2, b_1, b_3) S_t(x_2) \\
& \times \exp[-S_B(t_{dK}^1) - S_K(t_{dK}^1)|_{b_2 \rightarrow b_1} - S_\pi(t_{dK}^1)] + \alpha_s(t_{dK}^2) \left[ -(1 - x_3)(E_q - k_1^3) \phi_K(x_2, b_1) + r_K(1 - x_2) \right. \\
& \times (E_q + k_1^3) \phi_P^K(x_2, b_1) + \frac{1}{6} r_K(1 - x_2)(E_q + k_1^3) \phi_\sigma'^K(x_2, b_1) \Big] h_d(x_1, 1 - x_3, 1 - x_2, b_1, b_3) S_t(x_2) \\
& \left. \times \exp[-S_B(t_{dK}^2) - S_K(t_{dK}^2)|_{b_2 \rightarrow b_1} - S_\pi(t_{dK}^2)] \right\}. \tag{29}
\end{aligned}$$

The amplitudes of the nonfactorizable annihilation diagrams (e) and (f) are

$$\begin{aligned}
\mathcal{M}_a = & 2\pi^2 f_B f_K f_\pi m_B^2 \frac{C_F}{N_c} \int k_{1\perp} dk_{1\perp} \int_{x_1^d}^{x_1^u} dx_1 \int_0^1 dx_2 dx_3 \int_0^\infty b_1 db_1 b_2 db_2 \left( \frac{1}{2} m_B + \frac{|\mathbf{k}_{1\perp}|^2}{2x_1^2 m_B} \right) K(\vec{k}_1) (E_Q + m_Q) \\
& \times J_0(k_{1\perp} b_1) \left\{ \alpha_s(t_f^1) \left[ -x_3(E_q - k_1^3) \phi_K(x_2, b_2) \phi_\pi(x_3, b_2) - r_K r_\pi \left( (1 - x_2 + x_3)E_q + (1 - x_2 - x_3)k_1^3 \right) \right. \right. \\
& \times \phi_P^K(x_2, b_2) \phi_P^\pi(x_3, b_2) + \frac{1}{6} r_K r_\pi \left( (1 - x_2 - x_3)E_q + (1 - x_2 + x_3)k_1^3 \right) \phi_P^K(x_2, b_2) \phi_\sigma'^\pi(x_3, b_2) - \frac{1}{6} r_K r_\pi \\
& \times \left. \left. \left( (1 - x_2 - x_3)E_q + (1 - x_2 + x_3)k_1^3 \right) \phi_\sigma'^K(x_2, b_2) \phi_P^\pi(x_3, b_2) + \frac{1}{36} r_K r_\pi \left( (1 - x_2 + x_3)E_q + (1 - x_2 - x_3)k_1^3 \right) \phi_\sigma'^K(x_2, b_2) \phi_\sigma'^\pi(x_3, b_2) \right] h_f^1(1 - x_2, x_3, b_1, b_2) S_t(x_3) \exp[-S_B(t_f^1) - S_K(t_f^1) - S_\pi(t_f^1)|_{b_3 \rightarrow b_2}] \right. \\
& + \alpha_s(t_f^2) \left[ (1 - x_2)(E_q + k_1^3) \phi_K(x_2, b_2) \phi_\pi(x_3, b_2) + r_K r_\pi \left( (3 - x_2 + x_3)E_q + (1 - x_2 - x_3)k_1^3 \right) \right. \\
& \times \phi_P^K(x_2, b_2) \phi_P^\pi(x_3, b_2) + \frac{1}{6} r_K r_\pi \left( (1 - x_2 - x_3)E_q - (1 + x_2 - x_3)k_1^3 \right) \phi_P^K(x_2, b_2) \phi_\sigma'^\pi(x_3, b_2) \\
& \left. \left. - \frac{1}{6} r_K r_\pi \left( (1 - x_2 - x_3)E_q + (3 - x_2 + x_3)k_1^3 \right) \phi_\sigma'^K(x_2, b_2) \phi_P^\pi(x_3, b_2) + \frac{1}{36} r_K r_\pi \left( (1 + x_2 - x_3)E_q \right. \right. \right. \\
\end{aligned} \tag{30}$$

$$- (1 - x_2 - x_3) k_1^3 \Big) \phi_\sigma'^K(x_2, b_2) \phi_\sigma'^\pi(x_3, b_2) \Big] h_f^2(1 - x_2, x_3, b_1, b_2) \exp[-S_B(t_f^2) - S_K(t_f^2) - S_\pi(t_f^2)|_{b_3 \rightarrow b_2}] \Big\},$$

$$\begin{aligned} \mathcal{M}_a^P = & 2\pi^2 f_B f_K f_\pi m_B^2 \frac{C_F}{N_c} \int k_{1\perp} dk_{1\perp} \int_{x_1^d}^{x_1^u} dx_1 \int_0^1 dx_2 dx_3 \int_0^\infty b_1 db_1 b_2 db_2 \left( \frac{1}{2} m_B + \frac{|\mathbf{k}_{1\perp}|^2}{2x_1^2 m_B} \right) K(\vec{k}_1) (E_Q + m_Q) \\ & \times J_0(k_{1\perp} b_1) \left\{ \alpha_s(t_f^1) \left[ r_\pi x_3 (E_q + k_1^3) \phi_K(x_2, b_2) \phi_P^\pi(x_3, b_2) + \frac{1}{6} r_\pi x_3 (E_q + k_1^3) \phi_K(x_2, b_2) \phi_\sigma'^\pi(x_3, b_2) - r_K \right. \right. \\ & \times (1 - x_2) (E_q - k_1^3) \phi_P^K(x_2, b_2) \phi_\pi(x_3, b_2) + \frac{1}{6} r_K (1 - x_2) (E_q - k_1^3) \phi_\sigma'^K(x_2, b_2) \phi_\pi(x_3, b_2) \Big] \\ & \times h_f^1(1 - x_2, x_3, b_1, b_2) S_t(x_3) \exp[-S_B(t_f^1) - S_K(t_f^1) - S_\pi(t_f^1)|_{b_3 \rightarrow b_2}] + \alpha_s(t_f^2) \left[ r_\pi \left( (2 - x_3) E_q + x_3 k_1^3 \right) \right. \\ & \times \phi_K(x_2, b_2) \phi_P^\pi(x_3, b_2) + \frac{1}{6} r_\pi \left( (2 - x_3) E_q + x_3 k_1^3 \right) \phi_K(x_2, b_2) \phi_\sigma'^\pi(x_3, b_2) - r_K \left( (1 + x_2) E_q - (1 - x_2) k_1^3 \right) \\ & \times \phi_P^K(x_2, b_2) \phi_\pi(x_3, b_2) + \frac{1}{6} r_K \left( (1 + x_2) E_q - (1 - x_2) k_1^3 \right) \phi_\sigma'^K(x_2, b_2) \phi_\pi(x_3, b_2) \Big] h_f^2(1 - x_2, x_3, b_1, b_2) \\ & \times \exp[-S_B(t_f^2) - S_K(t_f^2) - S_\pi(t_f^2)|_{b_3 \rightarrow b_2}] \Big\}. \end{aligned} \quad (31)$$

In the Eqs. (20)–(31), we have defined

$$r_{K,\pi} = \mu_{K,\pi}/m_B = m_{K,\pi}^2/[(m_{s,u} + m_d)m_B], \quad (32)$$

$C_F = 4/3$  and  $N_c = 3$  are color factors. The function  $h$ 's are derived from the Fourier transformation of hard amplitudes.  $S_{B,K,\pi}(t)$  are Sudakov factors and  $S_t(x)$  is threshold factor. They are all given in Appendix A. The expressions of  $b$ -space wave functions  $\phi_K(x, b)$ ,  $\phi_P^K(x, b)$  and  $\phi_\sigma^K(x, b)$  can be found in Appendix B,  $\phi_\pi(x, b)$ ,  $\phi_P^\pi(x, b)$  and  $\phi_\sigma^\pi(x, b)$  can be found in Appendix of Ref. [24]. Particularly, the factor  $\chi_B$  in Eq. (25) is defined by

$$\begin{aligned} \chi_B = & \pi \int dk_{1\perp} k_{1\perp} \int_{x_1^d}^{x_1^u} dx_1 \left( \frac{1}{2} m_B + \frac{|\mathbf{k}_{1\perp}|^2}{2x_1^2 m_B} \right) \\ & \times K(\vec{k}_1) \left[ (E_q + m_q)(E_Q + m_Q) + |\vec{k}_1|^2 \right], \end{aligned} \quad (33)$$

which comes from the  $B$  to vacuum matrix element with the  $(S - P)$  operator inserted.

In order to decrease the high-order corrections, the renormalization scales  $t$  are taken as the largest virtualities in the decay amplitudes

$$\begin{aligned} t_e^1 = & \max(\sqrt{1 - x_3} m_B, 1/b_1, 1/b_3), \\ t_e^2 = & \max(\sqrt{x_1} m_B, 1/b_1, 1/b_3), \end{aligned} \quad (34)$$

$$t_{eK}^1 = \max(\sqrt{1 - x_2} m_B, 1/b_1, 1/b_2), \quad (35)$$

$$\begin{aligned} t_a^1 = & \max(\sqrt{x_3} m_B, 1/b_2, 1/b_3), \\ t_a^2 = & \max(\sqrt{1 - x_2} m_B, 1/b_2, 1/b_3), \end{aligned} \quad (36)$$

$$\begin{aligned} t_d^1 = & \max(\sqrt{x_1(1 - x_3)} m_B, \\ & \sqrt{x_2(1 - x_3)} m_B, 1/b_1, 1/b_2), \\ t_d^2 = & \max(\sqrt{x_1(1 - x_3)} m_B, \\ & \sqrt{(1 - x_2)(1 - x_3)} m_B, 1/b_1, 1/b_2), \end{aligned} \quad (37)$$

$$\begin{aligned} t_{dK}^1 = & \max(\sqrt{x_1(1 - x_2)} m_B, \\ & \sqrt{(1 - x_2)x_3} m_B, 1/b_1, 1/b_3), \\ t_{dK}^2 = & \max(\sqrt{x_1(1 - x_2)} m_B, \\ & \sqrt{(1 - x_2)(1 - x_3)} m_B, 1/b_1, 1/b_3), \end{aligned} \quad (38)$$

$$\begin{aligned} t_f^1 = & \max(\sqrt{(1 - x_2)x_3} m_B, 1/b_1, 1/b_2), \\ t_f^2 = & \max(\sqrt{(1 - x_2)x_3} m_B, \\ & \sqrt{1 - x_2 + x_2 x_3} m_B, 1/b_1, 1/b_2). \end{aligned} \quad (39)$$

In the language of the above matrix elements for different diagrams, i.e., Eqs. (20)–(31), the decay amplitudes for  $B \rightarrow K\pi$  decays can be written as:

$$\begin{aligned}
& \mathcal{M}(B^- \rightarrow \bar{K}^0 \pi^-) \\
&= -V_t \left( \frac{C_3}{N_c} + C_4 - \frac{1}{2} \frac{C_9}{N_c} - \frac{1}{2} C_{10} \right) f_K F_e - V_t \left( \frac{C_5}{N_c} + C_6 - \frac{1}{2} \frac{C_7}{N_c} - \frac{1}{2} C_8 \right) f_K F_e^P - \frac{V_t}{N_c} \left( C_3 - \frac{1}{2} C_9 \right) \mathcal{M}_e \\
&\quad - \frac{V_t}{N_c} \left( C_5 - \frac{1}{2} C_7 \right) \mathcal{M}_e^P + \frac{1}{N_c} \left[ V_u C_1 - V_t (C_3 + C_9) \right] \mathcal{M}_a - \frac{V_t}{N_c} (C_5 + C_7) \mathcal{M}_a^P \\
&\quad + \left[ V_u \left( \frac{C_1}{N_c} + C_2 \right) - V_t \left( \frac{C_3}{N_c} + C_4 + \frac{C_9}{N_c} + C_{10} \right) \right] f_B F_a - V_t \left( \frac{C_5}{N_c} + C_6 + \frac{C_7}{N_c} + C_8 \right) f_B F_a^P,
\end{aligned} \tag{40}$$

$$\begin{aligned}
& \sqrt{2} \mathcal{M}(B^- \rightarrow K^- \pi^0) \\
&= \left[ V_u \left( \frac{C_1}{N_c} + C_2 \right) - V_t \left( \frac{C_3}{N_c} + C_4 + \frac{C_9}{N_c} + C_{10} \right) \right] f_K F_e - V_t \left( \frac{C_5}{N_c} + C_6 + \frac{C_7}{N_c} + C_8 \right) f_K F_e^P \\
&\quad + \left[ V_u \left( C_1 + \frac{C_2}{N_c} \right) - \frac{3V_t}{2} \left( -C_7 - \frac{C_8}{N_c} + C_9 + \frac{C_{10}}{N_c} \right) \right] f_\pi F_{eK} + \frac{1}{N_c} \left[ V_u C_1 - V_t (C_3 + C_9) \right] \mathcal{M}_e \\
&\quad - \frac{V_t}{N_c} (C_5 + C_7) \mathcal{M}_e^P + \frac{1}{N_c} \left( V_u C_2 - \frac{3V_t}{2} C_{10} \right) \mathcal{M}_{eK} - \frac{V_t}{N_c} \frac{3}{2} C_8 \mathcal{M}_{eK}^P + \frac{1}{N_c} \left[ V_u C_1 - V_t (C_3 + C_9) \right] \mathcal{M}_a \\
&\quad - \frac{V_t}{N_c} (C_5 + C_7) \mathcal{M}_a^P + \left[ V_u \left( \frac{C_1}{N_c} + C_2 \right) - V_t \left( \frac{C_3}{N_c} + C_4 + \frac{C_9}{N_c} + C_{10} \right) \right] f_B F_a \\
&\quad - V_t \left( \frac{C_5}{N_c} + C_6 + \frac{C_7}{N_c} + C_8 \right) f_B F_a^P,
\end{aligned} \tag{41}$$

$$\begin{aligned}
& \mathcal{M}(\bar{B}^0 \rightarrow K^- \pi^+) \\
&= \left[ V_u \left( \frac{C_1}{N_c} + C_2 \right) - V_t \left( \frac{C_3}{N_c} + C_4 + \frac{C_9}{N_c} + C_{10} \right) \right] f_K F_e - V_t \left( \frac{C_5}{N_c} + C_6 + \frac{C_7}{N_c} + C_8 \right) f_K F_e^P \\
&\quad + \frac{1}{N_c} \left[ V_u C_1 - V_t (C_3 + C_9) \right] \mathcal{M}_e - \frac{V_t}{N_c} (C_5 + C_7) \mathcal{M}_e^P - \frac{V_t}{N_c} \left( C_3 - \frac{1}{2} C_9 \right) \mathcal{M}_a - \frac{V_t}{N_c} \left( C_5 - \frac{1}{2} C_7 \right) \mathcal{M}_a^P \\
&\quad - V_t \left( \frac{C_3}{N_c} + C_4 - \frac{1}{2} \frac{C_9}{N_c} - \frac{1}{2} C_{10} \right) f_B F_a - V_t \left( \frac{C_5}{N_c} + C_6 - \frac{1}{2} \frac{C_7}{N_c} - \frac{1}{2} C_8 \right) f_B F_a^P,
\end{aligned} \tag{42}$$

$$\begin{aligned}
& -\sqrt{2} \mathcal{M}(\bar{B}^0 \rightarrow \bar{K}^0 \pi^0) \\
&= -V_t \left( \frac{C_3}{N_c} + C_4 - \frac{1}{2} \frac{C_9}{N_c} - \frac{1}{2} C_{10} \right) f_K F_e - V_t \left( \frac{C_5}{N_c} + C_6 - \frac{1}{2} \frac{C_7}{N_c} - \frac{1}{2} C_8 \right) f_K F_e^P - \left[ V_u \left( C_1 + \frac{C_2}{N_c} \right) \right. \\
&\quad \left. - \frac{3V_t}{2} \left( -C_7 - \frac{C_8}{N_c} + C_9 + \frac{C_{10}}{N_c} \right) \right] f_\pi F_{eK} - \frac{V_t}{N_c} \left( C_3 - \frac{1}{2} C_9 \right) \mathcal{M}_e - \frac{V_t}{N_c} \left( C_5 - \frac{1}{2} C_7 \right) \mathcal{M}_e^P \\
&\quad - \frac{1}{N_c} \left( V_u C_2 - \frac{3V_t}{2} C_{10} \right) \mathcal{M}_{eK} + \frac{V_t}{N_c} \frac{3}{2} C_8 \mathcal{M}_{eK}^P - \frac{V_t}{N_c} \left( C_3 - \frac{1}{2} C_9 \right) \mathcal{M}_a - \frac{V_t}{N_c} \left( C_5 - \frac{1}{2} C_7 \right) \mathcal{M}_a^P \\
&\quad - V_t \left( \frac{C_3}{N_c} + C_4 - \frac{1}{2} \frac{C_9}{N_c} - \frac{1}{2} C_{10} \right) f_B F_a - V_t \left( \frac{C_5}{N_c} + C_6 - \frac{1}{2} \frac{C_7}{N_c} - \frac{1}{2} C_8 \right) f_B F_a^P,
\end{aligned} \tag{43}$$

with  $N_c = 3$ .

The decay width is calculated by

$$\Gamma(B \rightarrow K\pi) = \frac{G_F^2 m_B^3}{128\pi} |\mathcal{M}(B \rightarrow K\pi)|^2. \tag{44}$$

And the expressions of branching ratios and direct  $CP$  violations are

$$Br(B \rightarrow K\pi) = \Gamma(B \rightarrow K\pi) / \Gamma_B, \tag{45}$$

$$\begin{aligned}
& A_{CP}(B^0(B^+) \rightarrow K\pi) \\
&= \frac{\Gamma(\bar{B}^0(B^-) \rightarrow K\pi) - \Gamma(B^0(B^+) \rightarrow K\pi)}{\Gamma(\bar{B}^0(B^-) \rightarrow K\pi) + \Gamma(B^0(B^+) \rightarrow K\pi)}. \tag{46}
\end{aligned}$$

The Sudakov factor suppresses nonperturbative contributions and makes PQCD approach applicable [21, 22]. However, the suppression effect of Sudakov factor depends on the end-point behavior of wave functions. With the  $B$

meson wave function obtained by solving the bound-state equation in relativistic potential model [10–14], we find the suppression of Sudakov factor to soft contribution is not strong enough. To restore the reliability of perturbative calculation, we introduce the momentum cutoff and soft form factor in soft scale 1.0 GeV which corresponds to the strong coupling constant  $\alpha_s/\pi = 0.165$ . The contributions lower than the cutoff scale are removed and replaced by the relevant soft form factors. The effect of soft form factor will be investigated in Sec. IV.

### III. THE NEXT-TO-LEADING ORDER CORRECTIONS

In order to improve the results, the most important next-to-leading-order (NLO) corrections to the decay amplitudes from the vertex corrections, the quark loops, and the magnetic penguins are included. These contributions have been considered in PQCD approach in Ref. [2]. It turns out that the NLO corrections affect the amplitudes by changing the Wilson coefficients. For simplicity, we define the combinations of Wilson coefficients

$$\begin{aligned} a_1(\mu) &= C_2(\mu) + \frac{C_1(\mu)}{N_c}, \\ a_2(\mu) &= C_1(\mu) + \frac{C_2(\mu)}{N_c}, \\ a_i(\mu) &= C_i(\mu) + \frac{C_{i\pm 1}(\mu)}{N_c}, \end{aligned} \quad (47)$$

with  $i = 3 - 10$ . When  $i$  is odd (even), the plus (minus) sign is taken.

#### A. Vertex Corrections

At first, we consider the vertex corrections. Since the corrections of nonfactorizable diagrams are negligible and the annihilation diagrams themselves do not contribute much to the amplitudes, we concentrate on the vertex corrections of the factorizable emission diagrams, i.e., diagrams (a) and (b) in Fig. 1. The vertex corrections modify the Wilson coefficients as [2, 25–27]

$$\begin{aligned} a_1(\mu) &\rightarrow a_1(\mu) + \frac{\alpha_s(\mu)}{4\pi} C_F \frac{C_1(\mu)}{N_c} V_1(M), \\ a_2(\mu) &\rightarrow a_2(\mu) + \frac{\alpha_s(\mu)}{4\pi} C_F \frac{C_2(\mu)}{N_c} V_2(M), \\ a_i(\mu) &\rightarrow a_i(\mu) + \frac{\alpha_s(\mu)}{4\pi} C_F \frac{C_{i\pm 1}(\mu)}{N_c} V_i(M), \end{aligned} \quad (48)$$

with  $i = 3 - 10$ , and  $M$  represents the meson emitted from the weak vertex. For  $V_{1,4,6,8,10}$ ,  $M$  is kaon and for  $V_{2,3,5,7,9}$ ,  $M$  is pion. In the naive dimensional regularization (NDR) scheme  $V_i(M)$  are given by [25]

$$V_i(M) = \begin{cases} 12 \ln(m_b/\mu) - 18 + \int_0^1 dx \phi_M^A(x) g(x), & \text{for } i = 1 - 4, 9, 10 \\ -12 \ln(m_b/\mu) + 6 - \int_0^1 dx \phi_M^A(x) g(1-x), & \text{for } i = 5, 7 \\ -6 + \int_0^1 dx \phi_M^P(x) h(x), & \text{for } i = 6, 8 \end{cases} \quad (49)$$

with  $\phi_M^A(x)$  and  $\phi_M^P(x)$  are the twist-2 and twist-3 meson distribution amplitudes, and  $x$  the parton momentum fraction. The functions  $g(x)$  and  $h(x)$  are defined by

$$\begin{aligned} g(x) = & 3 \left( \frac{1-2x}{1-x} \ln x - i\pi \right) + \left[ 2\text{Li}_2(x) - \ln^2 x \right. \\ & \left. + \frac{2 \ln x}{1-x} - (3+2i\pi) \ln x - (x \longleftrightarrow 1-x) \right], \end{aligned} \quad (50)$$

$$h(x) = 2\text{Li}_2(x) - \ln^2 x - (1+2i\pi) \ln x - (x \longleftrightarrow 1-x). \quad (51)$$

#### B. Quark Loops

For the  $B \rightarrow K\pi$  decays, the effective Hamiltonian of the virtual quark loops are given by [2]

$$H_{\text{eff}} = - \sum_{q=u,c,t} \sum_{q'} \frac{G_F}{\sqrt{2}} V_{qb} V_{qs}^* \frac{\alpha_s(\mu)}{2\pi} C^{(q)}(\mu, l^2) \times (\bar{s}\gamma_\rho(1-\gamma_5)T^a b)(\bar{q}'\gamma^\rho T^a q'), \quad (52)$$

where  $l^2$  is the invariant mass of the gluon. The functions  $C^{(q)}(\mu, l^2)$  are

$$C^{(q)}(\mu, l^2) = \left[ G^{(q)}(\mu, l^2) - \frac{2}{3} \right] C_2(\mu), \quad (53)$$

for  $q = u, c$ , and

$$\begin{aligned} C^{(q)}(\mu, l^2) &= \left[ G^{(s)}(\mu, l^2) - \frac{2}{3} \right] C_3(\mu) \\ &+ \sum_{q''=u,d,s,c} G^{(q'')}(\mu, l^2) [C_4(\mu) + C_6(\mu)], \end{aligned} \quad (54)$$

for  $q = t$ . The function  $G^{(q)}(\mu, l^2)$  shown in Eq. (53) and (54) for the loop of the quark  $q$  is given by

$$\begin{aligned} G^{(q)}(\mu, l^2) &= -4 \int_0^1 dx x(1-x) \ln \frac{m_q^2 - x(1-x)l^2 - i\epsilon}{\mu^2}, \end{aligned} \quad (55)$$

where  $m_q$  is the quark mass.

Because the topological structure of quark loops is similar with the penguin diagrams, its effect can be absorbed into the Wilson coefficients  $a_4$  and  $a_6$  by

$$a_{4,6}(\mu) \rightarrow a_{4,6}(\mu) + \frac{\alpha_s(\mu)}{9\pi} \sum_{q=u,c,t} \frac{V_{qb}V_{qs}^*}{V_{tb}V_{ts}^*} C^{(q)}(\mu, \langle l^2 \rangle), \quad (56)$$

where  $\langle l^2 \rangle$  is the mean virtual gluon-momentum squared in the decay process. In our numerical calculations of  $B \rightarrow K\pi$  decays,  $\langle l^2 \rangle = m_b^2/4$  is taken as an average gluon momentum squared, which is a reasonable value in  $B$  decays.

### C. Magnetic Penguins

Then, we investigate the correction from the magnetic penguin. The effective Hamiltonian of the magnetic penguin contains the  $b \rightarrow sg$  transition

$$H_{\text{eff}} = -\frac{G_F}{\sqrt{2}} V_{tb} V_{ts}^* C_{8g} O_{8g}, \quad (57)$$

and the magnetic penguin operator is

$$O_{8g} = \frac{g_s}{8\pi^2} m_b \bar{s}_i \sigma_{\mu\nu} (1 + \gamma_5) T_{ij}^a G^{a\mu\nu} b_j, \quad (58)$$

with the color indices  $i$  and  $j$ . Considering the similar topological structure of magnetic penguin and quark loop, we can also absorb the contribution of magnetic penguin operator into the Wilson coefficients [2]

$$a_{4,6} \rightarrow a_{4,6} - \frac{\alpha_s(\mu)}{9\pi} \frac{2m_B}{\sqrt{\langle l^2 \rangle}} C_{8g}^{\text{eff}}(\mu), \quad (59)$$

with the effective Wilson coefficient  $C_{8g}^{\text{eff}} = C_{8g} + C_5$  [15].

## IV. THE CONTRIBUTION OF THE SOFT $BK$ , $B\pi$ TRANSITION AND $K\pi$ PRODUCTION FORM FACTORS

With Eqs. (20)-(31), we calculate the eight topological diagrams shown in Fig. 1 numerically, and find that soft contributions associated with diagrams (a), (b), (g) and (h) are not negligible. For the diagrams (a), (b), (g) and (h), there are more than 40% contributions in the range of  $\alpha_s/\pi > 0.2$  which are not in good perturbative region. In contrast, the soft contributions are only a few percent in diagrams (c), (d), (e) and (f). In order to improve the reliability of perturbative calculation, we introduce the momentum cutoff and soft form factors for scales lower than the critical scale  $\mu_c = 1.0$  GeV. That means we treat the contributions with the scale  $\mu < \mu_c$  as nonperturbative quantity and replace them by phenomenological soft form factors. The soft contributions are absorbed into two kinds of soft form factors, the  $BK$ ,

$B\pi$  transition form factors and the  $K\pi$  production form factor.

With the soft transition form factors, we can express the  $B \rightarrow K$  and  $B \rightarrow \pi$  transition form factors as

$$\begin{aligned} F_0^{BK} &= h_0^{BK} + \xi^{BK}, \\ F_0^{B\pi} &= h_0^{B\pi} + \xi^{B\pi}, \end{aligned} \quad (60)$$

where  $h_0^{BK}$  and  $h_0^{B\pi}$  represent the hard contributions which can be evaluated perturbatively in PQCD approach, and  $\xi^{BK}$  and  $\xi^{B\pi}$  are soft  $BK$ ,  $B\pi$  transition form factors. In result, the amplitudes in Eqs. (40)-(43) should be modified by

$$\begin{aligned} \mathcal{M}(B \rightarrow K\pi) &\rightarrow \mathcal{M}(B \rightarrow K\pi) \\ &- 2C_\pi(\mu_c) V_{CKM} f_\pi \xi^{BK} - 4r_\pi C'_\pi(\mu_c) V_{CKM} f_\pi \xi^{BK} \\ &- 2C_K(\mu_c) V_{CKM} f_K \xi^{B\pi} - 4r_K C'_K(\mu_c) V_{CKM} f_K \xi^{B\pi}, \end{aligned} \quad (61)$$

where  $V_{CKM}$  represents the relevant CKM matrix elements,  $r_{K,\pi}$  the parameters related with mesons kaon and pion which have been defined in Sec. II,  $C_\pi$  and  $C'_\pi$  the appropriate combinations of Wilson coefficients for the diagrams with pion emitted out and with  $(V-A)(V-A)$  and  $(S+P)(S-P)$  operators inserted respectively,  $C_K$  and  $C'_K$  are Wilson coefficients for kaon emitted diagrams. These Wilson coefficients are taken at the cutoff scale  $\mu_c$ , which is the critical separation scale of hard and soft contributions.

Furthermore, we also introduce the soft  $K\pi$  production form factor  $\xi^{K\pi}$  to absorb the soft contribution in factorizable annihilation diagrams (g) and (h) in Fig. 1. The  $K\pi$  form factor can be defined by the matrix element of scalar current

$$\langle K\pi | S | 0 \rangle = -\frac{1}{2} \sqrt{\mu_K \mu_\pi} F_+^{K\pi}, \quad (62)$$

where  $\mu_{K,\pi} = m_{K,\pi}^2/(m_{s,u} + m_d)$ . Considering the soft part, the  $K\pi$  production form factor can be written as

$$F_+^{K\pi} \rightarrow h^{K\pi} + \xi^{K\pi}, \quad (63)$$

where  $h^{K\pi}$  is the hard part that can be calculated perturbatively according to the factorizable annihilation diagrams, and  $\xi^{K\pi}$  the soft part of the  $K\pi$  production form factor. With the soft  $K\pi$  production form factor  $\xi^{K\pi}$ , the amplitudes are changed as

$$\begin{aligned} \mathcal{M}(B \rightarrow K\pi) &\rightarrow \\ \mathcal{M}(B \rightarrow K\pi) &- 2\sqrt{r_K r_\pi} C(\mu_c) V_{CKM} \chi_B f_B \xi^{K\pi}, \end{aligned} \quad (64)$$

where  $f_B$  is the decay constant of  $B$  meson,  $\chi_B$  the parameter defined in Eq. (33), and  $r_{K,\pi} = \mu_{K,\pi}/m_B$ .

## V. THE CONTRIBUTION OF COLOR-OCTET MATRIX ELEMENT

To improve the consistency between the theoretical calculation and experiment data, we take into account the

contribution from the hadronic matrix element of color-octet operators. By considering the relation for the generators of the color  $SU(3)$  group

$$T_{ik}^a T_{jl}^a = -\frac{1}{2N_c} \delta_{ik} \delta_{jl} + \frac{1}{2} \delta_{il} \delta_{jk}, \quad (65)$$

we can decompose the four-quark operators with any Dirac spinor structure into color-singlet and color-octet operators

$$\begin{aligned} & (\bar{q}_{1i} q_{2j})(\bar{q}_{3j} q_{4i}) \\ &= \frac{1}{N_c} (\bar{q}_{1i} q_{2i})(\bar{q}_{3j} q_{4j}) + 2(\bar{q}_{1i} T_{ik}^a q_{2k})(\bar{q}_{3j} T_{jl}^a q_{4l}), \end{aligned} \quad (66)$$

where the first and second terms correspond to color-singlet and -octet operators, respectively, and the specific Dirac spinor structure is omitted for simplicity.

For the  $B \rightarrow K\pi$  decays, at the leading order approximation, the hadronic matrix element of color-singlet operator can be written as

$$\begin{aligned} T_{K\pi}^0 &= \langle K\pi | (\bar{s}\gamma^\mu(1-\gamma_5)q)(\bar{q}\gamma_\mu(1-\gamma_5)b) | \bar{B} \rangle \\ &\approx -if_K m_B^2 F_0^{B\pi}(0), \\ T_{K\pi}^{SP0} &= \langle K\pi | (\bar{s}(1+\gamma_5)q)(\bar{q}(1-\gamma_5)b) | \bar{B} \rangle \\ &\approx -if_K r_K m_B^2 F_0^{B\pi}(0), \end{aligned} \quad (67)$$

where  $q \in \{u, d\}$ ,  $S$  and  $P$  stand for scalar and pseudoscalar currents. Whereas, up to now there is no reliable way to estimate the value for the color-octet hadronic matrix elements, which are defined as

$$\begin{aligned} T_{K\pi}^8 &= \langle K\pi | (\bar{s}T^a\gamma^\mu(1-\gamma_5)q)(\bar{q}T^a\gamma_\mu(1-\gamma_5)b) | \bar{B} \rangle, \\ T_{K\pi}^{SP8} &= \langle K\pi | (\bar{s}T^a(1+\gamma_5)q)(\bar{q}T^a(1-\gamma_5)b) | \bar{B} \rangle. \end{aligned} \quad (68)$$

In Eqs. (67) and (68), the quarks in the first current make up the first meson in the final state and the quarks in the second current involve the meson in the initial state and the second meson in the final state. Actually there should also be  $T_{\pi K}^{(SP)0}$  matrix elements in the calculation, but considering  $f_K F_0^{B\pi}(0) \approx f_\pi F_0^{BK}(0)$ , the difference between  $T_{K\pi}^{(SP)0}$  and  $T_{\pi K}^{(SP)0}$  can be safely neglected.

The color-octet hadronic matrix elements are usually dropped previously in the literature, because the hadronic states should be color-singlet. However, color-octet quark-antiquark states can change to be color-singlet states by exchanging soft gluons at distance of hadronic scale. Therefore, the contribution of the color-octet hadronic matrix element may not be zero from the theoretical point of view. In this work, we take the color-octet contributions into the consideration. With the approximation in Eq. (67), one can define the color-octet parameter  $\delta_8$  and  $\delta_8^{SP}$  through the color-octet hadronic matrix elements in the following way

$$\begin{aligned} T_{K\pi}^8 &= -if_K m_B^2 F_0^{B\pi}(0) \delta_8, \\ T_{K\pi}^{SP8} &= -if_K r_K m_B^2 F_0^{B\pi}(0) \delta_8^{SP}, \end{aligned} \quad (69)$$

so that  $\delta_8$  and  $\delta_8^{SP}$  can be viewed as a measure of how large the color-octet matrix element is compared to color-singlet matrix element. Including the color-octet contributions, the amplitudes in Eqs.(40)-(43) are modified by

$$\begin{aligned} \mathcal{M}(B^- \rightarrow \bar{K}^0 \pi^-) &\rightarrow \mathcal{M}(B^- \rightarrow \bar{K}^0 \pi^-) \\ &- \left[ -V_t \left( C_3 - \frac{1}{2} C_9 \right) \right] 4f_K F_0^{B\pi} \delta_8 \\ &- \left[ -V_t \left( C_5 - \frac{1}{2} C_7 \right) \right] 8r_k f_K F_0^{B\pi} \delta_8^{SP}, \end{aligned} \quad (70)$$

$$\begin{aligned} \sqrt{2} \mathcal{M}(B^- \rightarrow K^- \pi^0) &\rightarrow \sqrt{2} \mathcal{M}(B^- \rightarrow K^- \pi^0) \\ &- [V_u C_1 - V_t (C_3 + C_9)] 4f_K F_0^{B\pi} \delta_8 \\ &- [-V_t (C_5 + C_7)] 8r_k f_K F_0^{B\pi} \delta_8^{SP} \\ &- \left[ V_u C_2 - V_t \frac{3}{2} (-C_8 + C_{10}) \right] 4f_\pi F_0^{BK} \delta_8, \end{aligned} \quad (71)$$

$$\begin{aligned} \mathcal{M}(\bar{B}^0 \rightarrow K^- \pi^+) &\rightarrow \mathcal{M}(\bar{B}^0 \rightarrow K^- \pi^+) \\ &- [V_u C_1 - V_t (C_3 + C_9)] 4f_K F_0^{B\pi} \delta_8 \\ &- [-V_t (C_5 + C_7)] 8r_k f_K F_0^{B\pi} \delta_8^{SP}, \end{aligned} \quad (72)$$

$$\begin{aligned} -\sqrt{2} \mathcal{M}(\bar{B}^0 \rightarrow \bar{K}^0 \pi^0) &\rightarrow -\sqrt{2} \mathcal{M}(\bar{B}^0 \rightarrow \bar{K}^0 \pi^0) \\ &- \left[ -V_t \left( C_3 - \frac{1}{2} C_9 \right) \right] 4f_K F_0^{B\pi} \delta_8 \\ &- \left[ -V_t \left( C_5 - \frac{1}{2} C_7 \right) \right] 8r_k f_K F_0^{B\pi} \delta_8^{SP} \\ &+ \left[ V_u C_2 - V_t \frac{3}{2} (-C_8 + C_{10}) \right] 4f_\pi F_0^{BK} \delta_8. \end{aligned} \quad (73)$$

The value of color-octet parameters  $\delta_8$  and  $\delta_8^{SP}$  can be determined from experiment data. It is reasonable that the magnitude of them should not be too large.

## VI. NUMERICAL RESULT AND DISCUSSION

In addition to the parameters in  $B$  meson, pion and kaon wave functions, there are several other numerical parameters in the calculation, which are the soft  $BK$ ,  $B\pi$  transition form factors  $\xi^{BK}$  and  $\xi^{B\pi}$ , the soft  $K\pi$  production form factors  $\xi^{K\pi}$ , and the color-octet matrix element parameters  $\delta_8$  and  $\delta_8^{SP}$ .

The hard part of the  $BK$  and  $B\pi$  transition form factors  $h_0^{BK}$  and  $h_0^{B\pi}$  can be calculated directly in perturbative QCD with the momentum cutoff in scale  $\mu > 1.0$  GeV, which is relevant to the diagrams (a) and (b) in Fig. 1. The results of hard transition form factors are

$$\begin{aligned} h_0^{BK} &= 0.29 \pm 0.02, \\ h_0^{B\pi} &= 0.23 \pm 0.01. \end{aligned} \quad (74)$$

According to the experimental data and LCSR results, the total  $BK$  and  $B\pi$  transition form factors should be [16, 17]

$$\begin{aligned} F_0^{BK} &= 0.33 \pm 0.04, \\ F_0^{B\pi} &= 0.27 \pm 0.02. \end{aligned} \quad (75)$$

Using Eq. (60), we can determine that the soft part of the transition form factors are

$$\begin{aligned} \xi^{BK} &= 0.04 \pm 0.02, \\ \xi^{B\pi} &= 0.04 \pm 0.01. \end{aligned} \quad (76)$$

As for the color-octet parameters  $\delta_8$  and  $\delta_8^{SP}$ , there isn't a systematical way to evaluate the values of them. For simplicity, we assume they are at the same order and take

$$\delta_8 = \delta_8^{SP}. \quad (77)$$

The nonperturbative parameters  $\delta_8$  and  $\xi^{K\pi}$  can be written in the following form

$$\begin{aligned} \delta_8 &= d_1 \exp(i\phi_1), \\ \xi^{K\pi} &= d_2 \exp(i\phi_2), \end{aligned} \quad (78)$$

where  $d_{1,2}$  and  $\phi_{1,2}$  are the magnitudes and phases of these parameters, respectively. For  $B \rightarrow K\pi$  decays, there are data for branching ratios and  $CP$  violations of four decay modes, that can be used to determine these parameters. By fitting to the experimental data, we find the values of parameters are

$$\begin{aligned} d_1 &= 0.18^{+0.04}_{-0.06}, \quad \phi_1 = (-0.84^{+0.12}_{-0.12})\pi, \\ d_2 &= 0.039^{+0.016}_{-0.010}, \quad \phi_2 = (0.82^{+0.10}_{-0.07})\pi, \end{aligned} \quad (79)$$

where the uncertainties come from the constraint of experimental data. Using the parameters shown above, the predictions of  $B \rightarrow K\pi$  branching ratios and  $CP$  violations are

$$\begin{aligned} B(B^+ \rightarrow K^0\pi^+) &= 24.4^{+3.5+2.2}_{-4.6-2.2}, \\ B(B^+ \rightarrow K^+\pi^0) &= 12.6^{+1.6+0.9}_{-2.0-0.9}, \\ B(B^0 \rightarrow K^+\pi^-) &= 20.0^{+2.4+1.2}_{-3.3-1.3}, \\ B(B^0 \rightarrow K^0\pi^0) &= 9.4^{+1.3+0.8}_{-1.8-0.8}, \\ A_{CP}(B^+ \rightarrow K^0\pi^+) &= 0.008^{+0.001+0.001}_{-0.001-0.001}, \\ A_{CP}(B^+ \rightarrow K^+\pi^0) &= 0.052^{+0.033+0.011}_{-0.032-0.012}, \\ A_{CP}(B^0 \rightarrow K^+\pi^-) &= -0.080^{+0.014+0.030}_{-0.011-0.035}, \\ A_{CP}(B^0 \rightarrow K^0\pi^0) &= -0.124^{+0.037+0.020}_{-0.038-0.020}; \end{aligned} \quad (80)$$

where the first uncertainty comes from the uncertainties of the nonperturbative parameters in Eq. (79), and the second one from the uncertainties of the parameters in the meson wave functions.

The contributions of each theoretical component and the total results for the branching ratios and  $CP$  violations are listed in Table I. The experimental data are also

presented in the last column for comparison. In Table I, the column “NLO” means the hard contribution up to next-to-leading order in QCD, “+ $\xi^{BK(\pi)}$ ” the contribution of NLO plus the contribution of the soft transition form factor  $\xi^{BK}$  and  $\xi^{B\pi}$ , “+ $\xi^{K\pi}$ ” the contribution of NLO plus the contribution of soft production form factor of  $K\pi$ , “+ $T^8$ ” the contribution of NLO plus color-octet matrix element, and “+ $\xi^{BK(\pi)} + \xi^{K\pi} + T^8$ ” the total contribution of NLO+ $\xi^{BK(\pi)}$  +  $\xi^{K\pi}$  +  $T^8$ . As shown in Table I, the branching ratios of only hard calculation up to next-to-leading order are much smaller than experimental data. By introducing the soft  $BK$  and  $B\pi$  transition form factors  $\xi^{BK}$  and  $\xi^{B\pi}$ , the branching ratios are increased greatly, but the soft transition form factors only slightly affect  $CP$  violations. The soft  $K\pi$  production form factor  $\xi^{K\pi}$  reduces the branching ratios of these four decay channels by about 25%, but it does not affect  $CP$  violation too much either. The contribution of the color-octet matrix element  $T^8$  also increases the branching ratios by about 25%, which is similar as the effect of  $\xi^{K\pi}$ , but it can affect  $CP$  violation of  $B^+ \rightarrow K^+\pi^0$  significantly, which is the key point to solve the  $B \rightarrow K\pi$  puzzle. By comparing the last two columns of Table I, we can find that the theoretical results of all the branching ratios and most of the  $CP$  violations for  $B \rightarrow K\pi$  decays are consistent with the experiment data.  $CP$  violation for  $B^+ \rightarrow K^0\pi^+$  is very close to the data considering both the experimental and theoretical uncertainties.

## VII. SUMMARY

In this paper we study the  $B \rightarrow K\pi$  decays in a modified perturbative QCD approach. With the  $B$  meson wave function that is obtained in the relativistic potential model, we find that soft contribution can not be suppressed enough by Sudakov factor. It is necessary to introduce the soft scale cutoff and soft form factors. In addition, we also introduce the hadronic color-octet matrix element which plays an important role in explaining the dramatic difference between the  $CP$  violations of  $B^+ \rightarrow K^+\pi^0$  and  $B^0 \rightarrow K^+\pi^-$  decays. Taking appropriate values for the input parameters, our calculated results for all the branching ratios and  $CP$  violations of the  $B \rightarrow K\pi$  decay channels are consistent with the experimental data, except for the  $CP$  violation in the  $B^+ \rightarrow K^0\pi^+$  decay mode, which is very close to the experimental data.

## ACKNOWLEDGMENTS

This work is supported in part by the National Natural Science Foundation of China under Contracts No. 11875168.

TABLE I.  $B \rightarrow K\pi$  Branching Ratios and  $CP$  Violations.

Mode	NLO	$+\xi^{BK(\pi)}$	$+\xi^{K\pi}$	$+T^8$	$+\xi^{BK(\pi)} + \xi^{K\pi} + T^8$	Data[3]
$B(B^+ \rightarrow K^0\pi^+) \times 10^{-6}$	13.9	22.6	10.5	18.1	$24.4^{+3.5+2.2}_{-4.6-2.2}$	$(23.7 \pm 0.8)$
$B(B^+ \rightarrow K^+\pi^0) \times 10^{-6}$	8.5	13.2	6.5	9.6	$12.6^{+1.6+0.9}_{-2.0-0.9}$	$(12.9 \pm 0.5)$
$B(B^0 \rightarrow K^+\pi^-) \times 10^{-6}$	13.2	20.6	9.8	15.8	$20.0^{+2.4+1.2}_{-3.3-1.3}$	$(19.6 \pm 0.5)$
$B(B^0 \rightarrow K^0\pi^0) \times 10^{-6}$	5.2	8.6	3.8	7.2	$9.4^{+1.3+0.8}_{-1.8-0.8}$	$(9.9 \pm 0.5)$
$A_{CP}(B^+ \rightarrow K^0\pi^+)$	0.009	0.007	0.011	0.008	$0.008^{+0.001+0.001}_{-0.001-0.001}$	$-0.017 \pm 0.016$
$A_{CP}(B^+ \rightarrow K^+\pi^0)$	-0.039	-0.025	-0.027	0.039	$0.052^{+0.033+0.011}_{-0.032-0.012}$	$0.037 \pm 0.021$
$A_{CP}(B^0 \rightarrow K^+\pi^-)$	-0.105	-0.078	-0.104	-0.114	$-0.080^{+0.014+0.030}_{-0.011-0.035}$	$-0.083 \pm 0.004$
$A_{CP}(B^0 \rightarrow K^0\pi^0)$	-0.036	-0.032	-0.045	-0.140	$-0.124^{+0.037+0.020}_{-0.038-0.020}$	$0.00 \pm 0.13$

### Appendix A: Formulas in the Hard Part Calculations

The threshold factor  $S_t(x)$  is usually parameterized as

$$S_t(x) = \frac{2^{1+2c}\Gamma(3/2+c)}{\sqrt{\pi}\Gamma(1+c)}[x(1-x)]^c, \quad (\text{A1})$$

with  $c = 0.3$ .

The exponentials  $\exp[-S_{B,K,\pi}(t)]$  include the Sudakov factor and single ultraviolet logarithms which is related to the meson wave functions. The expressions of exponents are

$$S_B(t) = s(x_1, b_1, m_B) - \frac{1}{\beta_1} \ln \frac{\ln(t/\Lambda_{\text{QCD}})}{\ln(1/(b_1\Lambda_{\text{QCD}}))}, \quad (\text{A2})$$

$$S_K(t) = s(x_2, b_2, m_B) + s(1-x_2, b_2, m_B) - \frac{1}{\beta_1} \ln \frac{\ln(t/\Lambda_{\text{QCD}})}{\ln(1/(b_2\Lambda_{\text{QCD}}))}, \quad (\text{A3})$$

$$S_\pi(t) = s(x_3, b_3, m_B) + s(1-x_3, b_3, m_B) - \frac{1}{\beta_1} \ln \frac{\ln(t/\Lambda_{\text{QCD}})}{\ln(1/(b_3\Lambda_{\text{QCD}}))}. \quad (\text{A4})$$

The explicit form of  $s(x, b, Q)$  up to next-to-leading order is [28]

$$\begin{aligned} s(x, b, Q) = & \frac{A^{(1)}}{2\beta_1} \hat{q} \ln \left( \frac{\hat{q}}{\hat{b}} \right) - \frac{A^{(1)}}{2\beta_1} (\hat{q} - \hat{b}) + \frac{A^{(2)}}{4\beta_1^2} \left( \frac{\hat{q}}{\hat{b}} - 1 \right) - \left[ \frac{A^{(2)}}{4\beta_1^2} - \frac{A^{(1)}}{4\beta_1} \ln \left( \frac{e^{2\gamma_E-1}}{2} \right) \right] \ln \left( \frac{\hat{q}}{\hat{b}} \right) \\ & + \frac{A^{(1)}\beta_2}{4\beta_1^3} \hat{q} \left[ \frac{\ln(2\hat{q})+1}{\hat{q}} - \frac{\ln(2\hat{b})+1}{\hat{b}} \right] + \frac{A^{(1)}\beta_2}{8\beta_1^3} \left[ \ln^2(2\hat{q}) - \ln^2(2\hat{b}) \right] \\ & + \frac{A^{(1)}\beta_2}{8\beta_1^3} \ln \left( \frac{e^{2\gamma_E-1}}{2} \right) \left[ \frac{\ln(2\hat{q})+1}{\hat{q}} - \frac{\ln(2\hat{b})+1}{\hat{b}} \right] \\ & - \frac{A^{(1)}\beta_2}{16\beta_1^4} \left[ \frac{2\ln(2\hat{q})+3}{\hat{q}} - \frac{2\ln(2\hat{b})+3}{\hat{b}} \right] - \frac{A^{(1)}\beta_2}{16\beta_1^4} \frac{\hat{q}-\hat{b}}{\hat{b}^2} \left[ 2\ln(2\hat{b})+1 \right] \\ & + \frac{A^{(2)}\beta_2^2}{1728\beta_1^6} \left[ \frac{18\ln^2(2\hat{q})+30\ln(2\hat{q})+19}{\hat{q}^2} - \frac{18\ln^2(2\hat{b})+30\ln(2\hat{b})+19}{\hat{b}^2} \right] \\ & + \frac{A^{(2)}\beta_2^2}{432\beta_1^6} \frac{\hat{q}-\hat{b}}{\hat{b}^3} \left[ 9\ln^2(2\hat{b})+6\ln(2\hat{b})+2 \right], \end{aligned} \quad (\text{A5})$$

where  $\hat{q}$  and  $\hat{b}$  are defined as

$$\hat{q} \equiv \ln \left( xQ/(\sqrt{2}\Lambda_{\text{QCD}}) \right), \quad \hat{b} \equiv \ln(1/b\Lambda_{\text{QCD}}). \quad (\text{A6})$$

The coefficients  $\beta_i$  and  $A^{(i)}$  in Eq. (A5) are

$$\beta_1 = \frac{33-2n_f}{12}, \quad \beta_2 = \frac{153-19n_f}{24}, \quad (\text{A7})$$

and

$$\begin{aligned} A^{(1)} &= \frac{4}{3}, \\ A^{(2)} &= \frac{67}{9} - \frac{\pi^2}{3} - \frac{10}{27}n_f + \frac{8}{3}\beta_1 \ln\left(\frac{e^{\gamma_E}}{2}\right), \end{aligned} \quad (\text{A8})$$

where  $\gamma_E$  is Euler constant.

In the Eqs. (20)–(31), the function  $h$ 's are given as

$$\begin{aligned} h_e(x_1, x_2, b_1, b_2) &= K_0(\sqrt{x_1 x_2} m_B b_1) \left[ \theta(b_1 - b_2) K_0(\sqrt{x_2} m_B b_1) I_0(\sqrt{x_2} m_B b_2) \right. \\ &\quad \left. + \theta(b_2 - b_1) K_0(\sqrt{x_2} m_B b_2) I_0(\sqrt{x_2} m_B b_1) \right], \end{aligned} \quad (\text{A9})$$

$$\begin{aligned} h_a(x_1, x_2, b_1, b_2) &= K_0(-i\sqrt{x_1 x_2} m_B b_1) \left[ \theta(b_1 - b_2) K_0(-i\sqrt{x_2} m_B b_1) I_0(-i\sqrt{x_2} m_B b_2) \right. \\ &\quad \left. + \theta(b_2 - b_1) K_0(-i\sqrt{x_2} m_B b_2) I_0(-i\sqrt{x_2} m_B b_1) \right], \end{aligned} \quad (\text{A10})$$

$$\begin{aligned} h_d(x_1, x_2, x_3, b_1, b_2) &= K_0(-i\sqrt{x_2 x_3} m_B b_2) \left[ \theta(b_1 - b_2) K_0(\sqrt{x_1 x_3} m_B b_1) I_0(\sqrt{x_1 x_3} m_B b_2) \right. \\ &\quad \left. + \theta(b_2 - b_1) K_0(\sqrt{x_1 x_3} m_B b_2) I_0(\sqrt{x_1 x_3} m_B b_1) \right], \end{aligned} \quad (\text{A11})$$

$$\begin{aligned} h_f^1(x_1, x_2, b_1, b_2) &= K_0(-i\sqrt{x_1 x_2} m_B b_1) \left[ \theta(b_1 - b_2) K_0(-i\sqrt{x_1 x_2} m_B b_1) I_0(-i\sqrt{x_1 x_2} m_B b_2) \right. \\ &\quad \left. + \theta(b_2 - b_1) K_0(-i\sqrt{x_1 x_2} m_B b_2) I_0(-i\sqrt{x_1 x_2} m_B b_1) \right], \end{aligned} \quad (\text{A12})$$

$$\begin{aligned} h_f^2(x_1, x_2, b_1, b_2) &= K_0(\sqrt{x_1 + x_2 - x_1 x_2} m_B b_1) \left[ \theta(b_1 - b_2) K_0(-i\sqrt{x_1 x_2} m_B b_1) I_0(-i\sqrt{x_1 x_2} m_B b_2) \right. \\ &\quad \left. + \theta(b_2 - b_1) K_0(-i\sqrt{x_1 x_2} m_B b_2) I_0(-i\sqrt{x_1 x_2} m_B b_1) \right], \end{aligned} \quad (\text{A13})$$

where  $J_0$ ,  $K_0$  and  $I_0$  are Bessel and modified Bessel functions.

## Appendix B: Kaon Distribution Amplitudes

The transverse momentum dependence of  $\phi_K(x, k_\perp)$ ,  $\phi_P^K(x, k_\perp)$  and  $\phi_\sigma^K(x, k_\perp)$  is assumed to be a Gaussian distribution. When transform the wave function into  $b$ -space, the distribution amplitudes become

$$\phi(x, b) = \phi(x) \exp\left(-\frac{b^2}{4\beta^2}\right), \quad (\text{B1})$$

for  $\phi_K(x, b)$ ,  $\phi_P^K(x, b)$  and  $\phi_\sigma^K(x, b)$ . The twist-2 and twist-3 distribution amplitudes  $\phi_K(x)$ ,  $\phi_P^K(x)$  and  $\phi_\sigma^K(x)$  are given by [20]

$$\phi_K(x) = 6x(1-x) \left[ 1 + a_1^K C_1^{3/2}(t) + a_2^K C_2^{3/2}(t) \right], \quad (\text{B2})$$

$$\begin{aligned} \phi_P^K(x) &= 1 + a_0^P + a_1^P C_1^{1/2}(t) + a_2^P C_2^{1/2}(t) \\ &\quad + a_3^P C_3^{1/2}(t) + a_4^P C_4^{1/2}(t), \end{aligned} \quad (\text{B3})$$

$$\begin{aligned} \phi_\sigma^K(x) &= 6x(1-x) \left[ 1 + a_0^\sigma + a_1^\sigma C_1^{3/2}(t) \right. \\ &\quad \left. + a_2^\sigma C_2^{3/2}(t) + a_3^\sigma C_3^{3/2}(t) \right], \end{aligned} \quad (\text{B4})$$

where  $t = 2x - 1$ . The function  $C$ 's are Gegenbauer polynomials. The coefficients are

$$\begin{aligned} a_1^K(\mu = 1.0\text{GeV}) &= 0.06 \pm 0.03, \\ a_2^K(\mu = 1.0\text{GeV}) &= 0.25 \pm 0.15, \end{aligned} \quad (\text{B5})$$

$$\begin{aligned}
a_0^P(\mu = 1.0\text{GeV}) &= 0.58 \pm 0.23, \\
a_1^P(\mu = 1.0\text{GeV}) &= -0.57 \pm 0.31, \\
a_2^P(\mu = 1.0\text{GeV}) &= 0.79 \pm 0.25, \\
a_3^P(\mu = 1.0\text{GeV}) &= 0.18 \pm 0.12, \\
a_4^P(\mu = 1.0\text{GeV}) &= 0.06 \pm 0.04,
\end{aligned} \tag{B6}$$

$$\begin{aligned}
a_0^\sigma(\mu = 1.0\text{GeV}) &= 0.40 \pm 0.19, \\
a_1^\sigma(\mu = 1.0\text{GeV}) &= -0.13 \pm 0.09, \\
a_2^\sigma(\mu = 1.0\text{GeV}) &= 0.12 \pm 0.04, \\
a_3^\sigma(\mu = 1.0\text{GeV}) &= 0.03 \pm 0.01.
\end{aligned} \tag{B7}$$

---

[1] M. Beneke, M. Neubert, Nucl. Phys. B 675, 333 (2003).  
[2] H.N. Li, S. Mishima, and A.I. Sanda, Phys. Rev. D 72, 114005 (2005).  
[3] P.A. Zyla et al. (Particle Data Group), Prog. Theor. Exp. Phys. 2020, 083C01 (2020).  
[4] W. Bai, M. Liu, Y.Y. Fan, W.F. Wang, S. Cheng, and Z.J. Xiao, Chin. Phys. C 38, 033101 (2014).  
[5] H.N. Li and S. Mishima, Phys. Rev. D 83, 034023 (2011).  
[6] H.N. Li and S. Mishima, Phys. Rev. D 90, 074008 (2014).  
[7] A. Datta, J. Waite, and D. Sachdeva, Phys. Rev. D 100, 055015 (2019).  
[8] C. Kim, S. Oh, and Y.W. Yoon, Phys. Lett. B 665, 231 (2008).  
[9] S. Lü and M.Z. Yang, eprint arXiv:2211.10917.  
[10] M.Z. Yang, Eur. Phys. J. C 72, 1880 (2012).  
[11] J.B. Liu and M.Z. Yang, JHEP 2014, 106 (2014).  
[12] J.B. Liu and M.Z. Yang, Phys. Rev. D 91, 094004 (2015).  
[13] H.K. Sun and M.Z. Yang, Phys. Rev. D 95, 113001 (2017).  
[14] H.K. Sun and M.Z. Yang, Phys. Rev. D 99, 093002 (2019).  
[15] G. Buchalla, A.J. Buras, and M.E. Lautenbacher, Rev. Mod. Phys. 68, 1125 (1996).  
[16] A. Sibidanov et al. (Belle Collaboration), Phys. Rev. D 88, 032005 (2013).  
[17] P. Ball and R. Zwicky, Phys. Rev. D 71, 014015 (2005).  
[18] V.M. Braun and I. Filyanov, Z Phys. C 48, 239 (1990).  
[19] P. Ball, JHEP 01, 010 (1999).  
[20] P. Ball, V.M. Braun, and A. Lenz, JHEP 05, 004 (2006).  
[21] H.N. Li and H.L. Yu, Phys. Rev. D 53, 2480 (1996).  
[22] H.N. Li and H.L. Yu, Phys. Rev. D 53, 4970 (1996).  
[23] H.N. Li, Phys. Rev. D 66, 094010 (2002).  
[24] S. Lü and M.Z. Yang, Nucl. Phys. B 972, 115550 (2021).  
[25] M. Beneke, G. Buchalla, M. Neubert, and C.T. Sachrajda, Phys. Rev. Lett. 83, 1914 (1999).  
[26] M. Beneke, G. Buchalla, M. Neubert, and C.T. Sachrajda, Nucl. Phys. B 591, 313 (2000).  
[27] M. Beneke, G. Buchalla, M. Neubert, and C.T. Sachrajda, Nucl. Phys. B 606, 245 (2001).  
[28] H.N. Li, Phys. Rev. D 52, 3958 (1995).